



UNIVERSITY OF LEEDS

This is a repository copy of *Parahepatospora carcini* n. gen., n. sp., a parasite 1 of invasive *Carcinus maenas* with intermediate features of sporogony between the *Enterocytozoon* clade and other *Microsporidia*.

White Rose Research Online URL for this paper:
<http://eprints.whiterose.ac.uk/109600/>

Version: Accepted Version

Article:

Bojko, J, Clark, F, Bass, D et al. (4 more authors) (2017) *Parahepatospora carcini* n. gen., n. sp., a parasite 1 of invasive *Carcinus maenas* with intermediate features of sporogony between the *Enterocytozoon* clade and other *Microsporidia*. *Journal of Invertebrate Pathology*, 143. pp. 124-134. ISSN 0022-2011

<https://doi.org/10.1016/j.jip.2016.12.006>

© 2016 Published by Elsevier Inc. Licensed under the Creative Commons Attribution-NonCommercial-NoDerivatives 4.0 International
<http://creativecommons.org/licenses/by-nc-nd/4.0/>

Reuse

Unless indicated otherwise, fulltext items are protected by copyright with all rights reserved. The copyright exception in section 29 of the Copyright, Designs and Patents Act 1988 allows the making of a single copy solely for the purpose of non-commercial research or private study within the limits of fair dealing. The publisher or other rights-holder may allow further reproduction and re-use of this version - refer to the White Rose Research Online record for this item. Where records identify the publisher as the copyright holder, users can verify any specific terms of use on the publisher's website.

Takedown

If you consider content in White Rose Research Online to be in breach of UK law, please notify us by emailing eprints@whiterose.ac.uk including the URL of the record and the reason for the withdrawal request.



eprints@whiterose.ac.uk
<https://eprints.whiterose.ac.uk/>

1 **Parahepatospora carcini n. gen., n. sp., a parasite of invasive Carcinus maenas with**
2 **intermediate features of sporogony between the Enterocytozoon clade and other**
3 **Microsporidia**

4
5 Jamie Bojko^{1,2}, Fraser Clark³, David Bass^{2,4,5}, Alison M. Dunn¹, Sarah Stewart-Clark⁶, Paul
6 D. Stebbing⁷, Grant D. Stentiford^{2,4,*}

7
8 ¹Faculty of Biological Sciences, University of Leeds, Leeds, UK, LS2 9JT. ²Pathology and Molecular
9 Systematics Team, Centre for Environment, Fisheries and Aquaculture Science (Cefas), Weymouth
10 Laboratory, Weymouth, Dorset, UK, DT4 8UB. ³Department of Biomedical Sciences, University of
11 Prince Edward Island, Charlottetown, Prince Edward Island, Canada, C1A 4P3. ⁴European Union
12 Reference Laboratory for Crustacean Diseases, Centre for Environment, Fisheries and Aquaculture
13 Science (Cefas), Weymouth Laboratory, Weymouth, Dorset, UK, DT4 8UB. ⁵Department of Life
14 Sciences, Natural History Museum London, Cromwell Road, London, UK, SW7 5BD. ⁶Department of
15 Animal Science and Aquaculture, Dalhousie University Faculty of Agriculture, 58 River Road, Truro,
16 Nova Scotia, Canada, B2N 5E3. ⁷Epidemiology and Risk Team, Centre for Environment, Fisheries
17 and Aquaculture Science (Cefas), Weymouth Laboratory, Weymouth, Dorset, UK, DT4 8UB.

18
19
20 **Author e-mails:**

21 Jamie Bojko - bs09jb@leeds.ac.uk

22 Fraser Clark – fclark@mta.ca

23 David Bass – david.bass@cefas.co.uk

24 Alison M. Dunn – A.Dunn@Leeds.ac.uk

25 Sarah Stewart-Clark - Sarah.Stewart-Clark@Dal.Ca

26 Paul D. Stebbing – paul.stebbing@cefas.co.uk

27 Grant D. Stentiford (correspondence*) – grant.stentiford@cefas.co.uk

28 Tel: +44(0)1305 206722
29
30
31
32
33
34

35 **Abstract**

36 Parahepatospora carcini n. gen. n. sp., is a novel microsporidian parasite discovered
37 infecting the cytoplasm of epithelial cells of the hepatopancreas of a single Carcinus maenas
38 specimen. The crab was sampled from within its invasive range in Atlantic Canada (Nova
39 Scotia). Histopathology and transmission electron microscopy were used to show the
40 development of the parasite within a simple interfacial membrane, culminating in the
41 formation of unikaryotic spores with 5-6 turns of an isofilar polar filament. Formation of a
42 multinucleate meront (>12 nuclei observed) preceded thickening and invagination of the
43 plasmodial membrane, and in many cases, formation of spore extrusion precursors (polar
44 filaments, anchoring disk) prior to complete separation of pre-sporoblasts from the
45 sporogonial plasmodium. This developmental feature is intermediate between the
46 Enterocytozoonidae (formation of spore extrusion precursors within the sporont plasmodium)
47 and all other Microsporidia (formation of spore extrusion precursors after separation of
48 sporont from the sporont plasmodium). SSU rRNA-based gene phylogenies place P. carcini
49 within microsporidian Clade IV, between the Enterocytozoonidae and the so-called
50 Enterocytopora-clade, which includes Enterocytopora artemiae and Globulispora
51 mitoportans. Both of these groups contain gut-infecting microsporidians of aquatic
52 invertebrates, fish and humans. According to morphological and phylogenetic characters, we
53 propose that P. carcini occupies a basal position to the Enterocytozoonidae. We discuss the
54 discovery of this parasite from a taxonomic perspective and consider its origins and
55 presence within a high profile invasive host on the Atlantic Canadian coastline.

56

57 **Key words:** Abelspora; Phylogenetics; Enterocytozoonidae; Enterocytopora; Taxonomy;
58 Invasive-Pathogens

59

60

61

62

63

64

65

66

67

68

69

70

71

72

73

74 **1. Introduction**

75 Microsporidia are a highly diverse group of obligate intracellular parasites, belonging to a
76 sister clade to the Fungi Kingdom, which also includes the Aphelids and Cryptomycota
77 (Haag et al. 2014; Corsaro et al. 2014; Karpov et al. 2015). Their diversity remains highly
78 under-sampled, but known microsporidia infect a wide array of host taxa, many of which
79 occur in aquatic habitats (Stentiford et al. 2013). Molecular-phylogenetic approaches are not
80 only clarifying the position of the Microsporidia amongst the eukaryotes, but are also
81 increasingly defining within-phylum taxonomy (Stentiford et al. 2016).

82

83 Microsporidian phylogenies built upon ribosomal gene sequence data have led to proposals
84 for five taxonomically distinctive microsporidian clades (I, II, III, IV, V), each of which can be
85 further aligned to three broad ecological groupings; the Marinosporidia (V); Terresporidia (II,
86 IV); and Aquasporidia (I, III) (Vossbrinck and Debrunner-Vossbrinck, 2005). Clade IV forms a
87 particularly interesting group due to the fact that it contains the family Enterocytozoonidae,
88 where all known taxa infect aquatic invertebrates or fish hosts; with the exception of a single
89 species complex (*Enterocytozoon bieneusi*). *Enterocytozoon bieneusi* is the most common
90 microsporidian pathogen infecting immune-suppressed humans (Stentiford et al. 2013;
91 Stentiford et al. 2016). Other genera within the Enterocytozoonidae include: *Desmozoon*
92 (=Paranucleospora), *Obruspora*, *Nucleospora*, and *Enterospora*. Other species, such as
93 *Enterocytozoon hepatopenaei*, which infect fish and shrimp, appear to have been assigned
94 to the genus *Enterocytozoon* erroneously, using relatively low SSU sequence similarity
95 (~88%) and similar development pattern contrary to a closer SSU sequence similarity to the
96 *Enterospora* genus (~93%) (Tourtip et al. 2009). Based upon its phylogenetic position, *E.*
97 *bieneusi* is almost certainly a zoonotic pathogen of humans, likely with origins in aquatic
98 habitats (Stentiford et al. 2016). This makes the phylogeny of existing and novel
99 microsporidians within, and related to, the family Enterocytozoonidae is an intriguing
100 research topic. Aquatic crustaceans may offer a likely evolutionary origin to current day
101 human infections by *E. bieneusi* (Stentiford et al. 2016).

102

103 The microsporidium *Hepatospora eriocheir* was recently discovered infecting the
104 hepatopancreas of aquatic crustaceans (Stentiford et al. 2011; Bateman et al. 2016).
105 Morphological characters and phylogenetic analysis found that *H. eriocheir* was related to
106 the Enterocytozoonidae; grouping as a sister group to this family on SSU rRNA gene trees
107 (Stentiford et al. 2011). *Hepatospora eriocheir* displayed somewhat intermediate characters
108 between the Enterocytozoonidae and all other known taxa (e.g. potential to form spore

109 extrusion precursors in bi-nucleate sporonts prior to their separation and, to uninucleate
110 sporoblast and spore formation) even though the distinctive morphological characters of the
111 Enterocytozoonidae were not observed (e.g. presence of spore extrusion precursors in multi-
112 nucleate sporonts). Spore extrusion precursors develop after final separation of pre-
113 sporoblasts from sporont plasmodia in all other microsporidians. The discovery of the genus
114 Hepatospora led our laboratory to propose a sister family to the Enterocytozoonidae with
115 intermediate traits between this family and other existing taxa. The family was tentatively
116 assigned as the Hepatosporidae with *H. eriocheir* (and the newly erected genus
117 Hepatospora), as its type member, pending discovery of further members (Stentiford et al.
118 2011).

119
120 This study describes a novel microsporidian infecting the hepatopancreas of *Carcinus*
121 *maenas* (European shore crab, or invasive green crab), commonly referred to as the green
122 crab in North America, collected from within its invasive range in Nova Scotia, Canada as
123 part of ongoing studies to investigate diversity and origins of the families Enterocytozoonidae
124 and Hepatosporidae in aquatic invertebrate hosts. We determined that this parasite falls at
125 the base of the Enterocytozoonidae, Enterocytozoon-like clade and the tentatively proposed
126 Hepatosporidae based upon morphological, ultrastructural and phylogenetic evidence. The
127 new parasite is distinct from *Abelspora portucalensis* (a previously described microsporidian
128 infecting the hepatopancreas of *C. maenas*, but without available genetic data), and three
129 other microsporidians, known to infect *C. maenas* from its native range in Europe (Sprague
130 and Couch, 1971; Azevedo, 1987; Stentiford et al. 2013). Given that the new parasite was
131 not discovered within its host's native range, it is possible that it represents a case of
132 parasite acquisition from the host community in which this non-native crab now resides. We
133 erect the genus *Parahepatospora* n. gen. and species *Parahepatospora carcini* n. sp. to
134 contain this novel parasite.

135

136 **2. Materials and Methods**

137 2.1 Sample collection

138 *Carcinus maenas* were sampled from Malagash Harbour on the north shore of Nova Scotia,
139 Canada (45.815154, -63.473768) on 26/08/2014 using a mackerel-baited Nickerson green
140 crab trap. In total, 134 *C. maenas* were collected from this site and transported to the
141 Dalhousie University Agricultural Campus where they were kept overnight in damp
142 conditions. Animals were euthanized, then necropsied with muscle, hepatopancreas, heart,
143 gonad and gill tissue, preserved for DNA extraction (100% ethanol), transmission electron
144 microscopy (2.5% glutaraldehyde) and histopathology (Davidson's saltwater fixative) using

145 protocols defined by the European Union Reference Laboratory for Crustacean Diseases
146 (www.crustaceancrl.eu).

147

148 2.2 Histology

149 Tissues were submerged in Davidson's saltwater fixative (Hopwood, 1996) for 24-48 hours
150 then immersed in 70% ethanol prior to transportation to the Cefas Weymouth Laboratory,
151 UK. Samples were prepared for histological analysis by wax infiltration using a robotic tissue
152 processor (Peloris, Leica Microsystems, United Kingdom) before being embedded into wax
153 blocks. Specimens were sectioned a single time at 3-4µm (Finesse E/NE rotary microtome)
154 and placed onto glass slides, prior to staining with haematoxylin and alcoholic eosin (H&E).
155 Data collection and imaging took place on a Nikon-integrated Eclipse (E800) light
156 microscope and digital imaging software at the Cefas laboratory (Weymouth).

157

158 2.3 Transmission electron microscopy (TEM)

159 Glutaraldehyde-fixed tissue biopsies were soaked in sodium cacodylate buffer twice (10 min)
160 and placed into 1% Osmium tetroxide (OsO₄) solution for 1 hour. Osmium stained material
161 underwent an acetone dilution series as follows: 10% (10 min); 30% (10 min); 50% (10 min);
162 70% (10 min); 90% (10 min); 100% (x3) (10 min). Samples were then permeated with
163 Agar100 Resin using a resin:acetone dilution series: 1:4; 1:1; 4:1; 100% resin (x2). Each
164 sample was placed into a cylindrical mould (1 cm³) along with fresh resin and polymerised in
165 an oven (60°C) for 16 hours. The resulting blocks were cropped to expose the tissue using a
166 razor blade and sectioned at 1µm thickness (stain: Toluidine Blue) using a glass knife before
167 being read on an Eclipse E800 light microscope to confirm infection. Ultra-thin sections were
168 taken at ~80nm thickness using a diamond knife, stained with uranyl acetate and Reynolds
169 lead citrate (Reynolds, 1963), and read/annotated on a Jeol JEM 1400 transmission electron
170 microscope (Jeol, UK).

171

172 2.4 PCR and sequencing

173 DNA was extracted from ethanol-fixed samples of hepatopancreas using an automatic EZ1
174 DNA extraction kit (Qiagen). Primers: MF1 (5'-CCGGAGAGGGAGCCTGAGA-3') and MR1
175 (5'-GACGGGCGGTGTGTACAAA-3') (Tourtip et al. 2009), were used to amplify a fragment
176 of the microsporidian SSU rRNA gene using a GoTaq flexi PCR reaction [1.25U of Taq
177 polymerase, 2.5mM MgCl₂, 0.25mM of each dNTP, 100pMol of each primer and 2.5µl of
178 DNA template (10-30ng/µl) in a 50µl reaction volume]. Thermocycler settings were as
179 follows: 94°C (1 min) followed by 30 cycles of 94°C (1 min), 55°C (1 min), 72°C (1 min) and
180 then a final 72°C (10 min) step. Electrophoresis through a 2% Agarose gel (120V, 45min)
181 was used to separate and visualise a resulting 939bp amplicon. Amplicons were purified

182 from the gel and sent for forward and reverse DNA sequencing (Eurofins genomics
183 sequencing services: <https://www.eurofinsgenomics.eu/>).

184

185 2.5 Phylogenetic tree construction

186 Several microsporidian sequences were downloaded from NCBI (GenBank), biased towards
187 clade IV (Vossbrinck and Debrunner-Vossbrinck, 2005), but also including members of clade
188 III, and the genus *Glugea* (clade V) as an out-group. BLASTn searches were used to retrieve
189 the closest related sequences to the *C. maenas* parasite. The consensus sequence of the
190 SSU rRNA gene of the new parasite (939nt) was added and aligned with the aforementioned
191 dataset using the E-ins-I algorithm within mafft version 7 (Kato and Standley, 2013). The
192 resulting alignment, (65 sequences, 1812 positions analysed) was refined manually and
193 analysed firstly using Maximum Likelihood (ML) in RAxML BlackBox version 8 (Stamatakis,
194 2014) [Generalized time-reversible (GTR) model with CAT approximation (all parameters
195 estimated from the data)]; an average of 10,000 bootstrap values was mapped onto the tree
196 with the highest likelihood value. A Bayesian consensus tree was then constructed using
197 MrBayes v3.2.5 for a secondary comparative tree (Ronquist et al. 2012). Two separate MC³
198 runs with randomly generated starting trees were carried out for 5 million generations, each
199 with one cold and three heated chains. The evolutionary model used by this study included a
200 GTR substitution matrix, a four-category auto-correlated gamma correction, and the covarion
201 model. All parameters were estimated from the data. Trees were sampled every 1,000
202 generations. The first 1.25 M generations were discarded as burn-in (trees sampled before
203 the likelihood plots reached stationarity) and a consensus tree was constructed from the
204 remaining sample. The 18S rDNA sequence generated by this study is available from NCBI
205 (accession number: KX757849).

206

207

208 **3. Results**

209 3.1 Histopathology

210 Of the 134 individuals sampled from the shoreline at Malagash, a single individual (trap-
211 caught male) was found to be parasitized by a microsporidian parasite targeting the
212 epithelial cells of the hepatopancreatic tubules (1/134; <1%). At the time of dissection, the
213 hepatopancreas of the infected individual appeared to be healthy without clearly-visible
214 clinical signs of infection at the time of necropsy. Histopathological analysis revealed the
215 microsporidian infection to be contained within the cytoplasm of infected
216 hepatopancreatocytes (Fig. 1a-c). Presumed early life stages of the parasites (meronts and
217 sporont plasmodia) stained dark blue/purple under H&E whilst apparent later life stages
218 (sporoblasts, spores) became eosinophilic and refractile (Fig. 1b). In general, early life-

219 stages of the parasite were observed to develop at the periphery of the infected cell while
220 spores generally occupied more central positions (Fig. 1b). In late stages of cellular
221 colonisation, infected host cells appeared to lose contact with neighbour cells and the
222 basement membrane for presumed expulsion to the tubule lumen (hepatopancreatic tubules
223 empty to the intestine) (Fig. 1c). Infected hepatopancreatic tubules appeared heavily
224 degraded during late stage infection due to the sloughing of infected cells from the basal
225 membrane (Fig. 1a-c).

226

227 3.2 Microsporidian ultrastructure and proposed lifecycle

228 All stages of the microsporidian parasite occurred within a simple interfacial membrane,
229 which separated parasite development stages from the host cell cytoplasm. Earliest
230 observed life stages, apparent uninucleate meronts, contained a thin cell membrane and
231 were present at the periphery of the interfacial membrane (Fig. 2a). Unikaryotic meronts
232 appeared to undergo nuclear division without cytokinesis, leading to a diplokaryotic meront,
233 again occurring predominantly at the periphery of the interfacial membrane (Fig. 2b).
234 Darkening of the diplokaryotic cell cytoplasm and separation of the adjoined nuclei, possibly
235 via nuclear dissociation, preceded further nuclear divisions to form multinucleate meronts,
236 with the greatest number of (visible) nuclei observed being 12 (Fig. 2c-d). The multinucleate
237 plasmodia appear to invaginate and elongate (Fig. 2d). Following thickening of the
238 multinucleate plasmodial wall, primary spore organelle formation (polar filament and
239 anchoring disk precursors) occurred prior to the separation of pre-sporoblasts from the
240 sporont plasmodium in most cases (primary pathway); only in a few cases were spore pre-
241 cursor organelles not present (Fig. 2 e-f). Other sporonts appeared to progress to
242 sporoblasts by forming precursor spore organelles after separation from the multinucleate
243 sporont plasmodium. Each sporoblast contained a single nucleus (Fig. 2f). Sporoblasts
244 displayed noticeable thickening of the endospore and electron lucent zones of their walls
245 (Fig. 3a). Mature spores contained an electron dense cytoplasm and were oval shaped with
246 a length of $1.50\mu\text{m} \pm 0.107\mu\text{m}$ (n=10) and a width of $1.12\mu\text{m} \pm 0.028\mu\text{m}$ (n=16). Spores
247 were unikaryotic, and possessed a relatively thin spore wall, consisting of a thin endospore
248 [$39.21\text{nm} \pm 8.674$ (n=30)], exospore [$26.47\text{nm} \pm 2.301\text{nm}$ (n=30)] and internal cell
249 membrane. The polar filament was layered with electron lucent and electron dense rings
250 resulting in an overall diameter of $64.18\text{nm} \pm 5.495\text{nm}$ (n=22). The polar filament underwent
251 5 to 6 turns (Fig. 3b-d) and was terminated with an anchoring disk [width: $292.20\text{nm} \pm$
252 19.169nm (n=5)]. The endospore appeared slightly thinner in the vicinity of the anchoring
253 disk. A highly membranous polaroplast and electron lucent polar vacuole were observed at
254 the anterior and posterior of the spore, respectively (Fig. 3b-d). A depiction of the full
255 lifecycle is presented in Fig. 4.

256
257
258
259
260
261
262
263
264
265
266
267
268
269
270
271
272
273
274
275
276
277
278
279
280
281
282
283
284
285
286
287
288
289
290
291
292

3.3 Phylogeny of the novel microsporidian infecting *C. maenas*

A single consensus DNA sequence (939bp) from the microsporidian parasite was obtained and utilised to assess the phylogeny of the novel taxon. BLASTn results revealed the highest scored hit belonged to *Globulispora mitoportans* (KT762153.1; 83% identity; 99% coverage; total score = 815; e-value = 0.0). The closest overall identity match belonged to 'Microsporidium sp. BPAR2 TUB1' (FJ756098.1; 85% identity; 57% coverage; total score = 527; e-value = 2e-145). This suggested that the new parasite belonged in Clade IV of the Microsporidia (Vossbrinck and Debrunner-Vossbrinck, 2005) but, with distinction from all described taxa to date.

Maximum Likelihood (ML) and Bayesian (Pp) analyses grouped the new parasite within Clade IV of the microsporidia and positioned it basally to the Enterocytozoonidae, Enterocytopora-like clade, putative Hepatosporidiae and other taxonomic families (indicated on Fig. 5), at weak confidence: 0.30 (ML) and 0.53 (Pp) (Fig. 5). This provides us with a rough estimate of its phylogeny but with little confidence as to its true position and association to the families represented in the tree.

A second tree representing microsporidian taxa that have been taxonomically described (including developmental, morphological and SSU rDNA sequence data) is presented in Fig. 6. This tree is annotated with developmental traits at the pre-sporoblastic (sporont) divisional level and identifies that *H. eriocheir* and *P. carcini* show intermediate development pathways between the Enterocytozoonidae and the Enterocytopora-like clade, supported weakly [0.38 (ML), 0.42 (Pp)] by the 18S phylogenetics. *Parahepatospora carcini* branched between the formally described *Agmasoma penaei* and *H. eriocheir*: both parasites of Crustacea but each with different developmental strategies at the pre-sporoblastic level (Fig. 6).

4 Taxonomic description

4.1 Higher taxonomic rankings

Super-group: Opisthokonta

Super-Phylum: Opisthosporidia (Karpov et al. 2015)

Phylum: Microsporidia (Balbiani, 1882)

Class: Terresporidia (Clade IV) (*nomina nuda*) (Vossbrinck and Debrunner-Vossbrinck, 2005)

293 4.2 Novel taxonomic rankings

294 Genus: *Parahepatospora* (Bojko, Clark, Bass, Dunn, Stewart-Clark, Stebbing, Stentiford
295 gen. nov.)

296 Genus description: Morphological features are yet to be truly defined as this is currently a
297 monotypic genus. Developmental characteristics may include: polar-filament development
298 prior to budding from the multinucleate plasmodium; multinucleate cell formation; nuclear
299 division without cytokinesis at the meront stage; and budding from a plasmodial filament,
300 would increase the confidence of correct taxonomic placement. Importantly, sporonts (pre-
301 sporoblasts) have the capacity to develop precursors of the spore extrusion apparatus prior
302 to their separation from the sporont plasmodium. Novel taxa placed within this genus will
303 likely have affinity to infect the hepatopancreas (gut) of their host and clade closely to the
304 type species *P. carcini* (accession number: KX757849 serves as a reference sequence for
305 this genus).

306

307 Type species: *Parahepatospora carcini* (Bojko, Clark, Bass, Dunn, Stewart-Clark, Stebbing,
308 Stentiford sp. nov.)

309 Description: All life stages develop within a simple interfacial membrane in the cytoplasm of
310 host cells. Spores appear oval shaped (L: $1.5\mu\text{m} \pm 0.107\mu\text{m}$, W: $1.1\mu\text{m} \pm 0.028\mu\text{m}$), and
311 have an electron lucent endospore (thickness: $39.21\text{nm} \pm 8.674\text{nm}$) coupled with an electron
312 dense exospore (thickness: $26.47\text{nm} \pm 2.3\text{nm}$) by TEM. The polar filament turns 5-6 times
313 and the polaroplast of the spore is highly membranous. The spores are unikaryotic with
314 unikaryotic merogonic stages during early development, which progress through a
315 diplokaryotic meront stage to a multinucleate plasmodium stage in which spore extrusion
316 precursors primarily form prior to the separation of sporonts (pre-sporoblasts). Sporonts bud
317 from the plasmodium via an elongation of the cytoplasm. *Parahepatospora carcini* SSU
318 rDNA sequence data is represented by accession number: KX757849.

319

320 Type host: *Carcinus maenas*, Family: Portunidae. Common names include: European shore
321 crab and invasive green crab.

322

323 Type locality: Malagash (invasive range) (Canada, Nova Scotia) (45.815154, -63.473768).

324

325 Site of infection: Cytoplasm of hepatopancreatocytes.

326

327 Etymology: “*Parahepatospora*” is named in accordance to the genus “*Hepatospora*” based
328 upon a similar tissue tropism (hepatopancreas) and certain shared morphological

329 characters. The specific epithet “*carcini*” refers to the type host (*Carcinus maenas*) in which
330 the parasite was detected.

331

332 Type material: Histological sections and TEM resin blocks from the infected Canadian
333 specimen is deposited in the Registry of Aquatic Pathology (RAP) at the Cefas Weymouth
334 Laboratory, UK. The SSU rRNA gene sequence belonging to *P. carcini* has been deposited
335 in Gen-Bank (NCBI) (accession number: KX757849).

336

337

338 **5 Discussion**

339 This study describes a novel microsporidian parasite infecting the hepatopancreas of a
340 European shore crab (*Carcinus maenas*), from an invasive population in Atlantic Canada
341 (Malagash, Nova Scotia). Our SSU rRNA phylogenies place *Parahepatospora carcini* within
342 Clade IV of the Microsporidia, and specifically at the base of the Enterocytozoonidae
343 (containing *Enterocytozoon bieneusi*) and recently-described Enterocytozoon-like clade
344 (infecting aquatic invertebrates) (Vavra et al. 2016). Its appearance at the base of these
345 clades coupled with its host pathology and development, suggest that this species falls
346 within the Hepatosporidae. However, this cannot be confirmed with current genetic and
347 morphological data. Collection of further genetic data in the form of more genes from both
348 this novel species and other closely related species, will help to infer a more confident
349 placement in future. *Parahepatospora carcini* is morphologically distinct from the
350 microsporidian *Abelspora portucalensis*, which parasitizes the hepatopancreas of *C. maenas*
351 from its native range in Europe (Azevedo, 1987). It is important here to consider whether *P.*
352 *carcini* has been acquired in the invasive range of the host, or whether this novel
353 microsporidian is an invasive pathogen carried by its host from its native range.

354

355 5.1 Could *Parahepatospora carcini* n. gen. n. sp. be *Abelspora portucalensis* (Azevedo,
356 1987)?

357 *Abelspora portucalensis* was initially described as a common microsporidian parasite of *C.*
358 *maenas* native to the Portuguese coast (Azevedo, 1987). While *A. portucalensis* and *P.*
359 *carcini* infect the same organ (hepatopancreas), and both develop within interfacial
360 membranes separating them from the cytoplasm of infected cells, the two parasites do not
361 resemble one another morphologically. No visible pathology was noted for *P. carcini*
362 whereas *A. portucalensis* leads to the development of ‘white cysts’ on the surface of the
363 hepatopancreas, visible upon dissection. In contrast to the high prevalence of *A.*
364 *portucalensis* in crabs collected from the Portuguese coast, *P. carcini* infection was rare
365 (<1%) in crabs collected from the Malagash site (this study).

366

367 The parasites share some ultrastructural characteristics, such as: a uninucleate spore with
368 5-6 turns of a polar filament and a thin endospore. However, the ellipsoid spore of each
369 species shows dissimilar dimensions [*A. portucalensis* (L: “3.1 - 3.2 μ m”, W: “1.2 – 1.4 μ m”)
370 Azevedo, 1987] [*P. carcini* (L: 1.5 μ m \pm 0.107 μ m, W: 1.1 μ m \pm 0.028 μ m)]. In addition, *A.*
371 *portucalensis* spores were observed to develop in pairs, within a sporophorous vesicle whilst
372 life stages of *P. carcini* develop asynchronously within an interfacial membrane (Fig. 2-3).
373 *Parahepatospora carcini* undergoes nuclear division to form a diplokaryotic meront without
374 cytokinesis (Fig. 2b) where both *A. portucalensis* and *H. eriocheir* undergo nuclear division
375 with cytokinesis at this developmental step; further distinguishing these two species from *P.*
376 *carcini*. *Parahepatospora carcini* also possesses a characteristically distinctive development
377 stage in which multinucleate plasmodia lead to the production of early sporoblasts. These
378 sporoblasts develop spore extrusion organelles prior to their separation from the
379 plasmodium (Fig. 2 e-f). This critical developmental step, characteristic of all known
380 members of the Enterocytozoonidae (Stentiford et al. 2007) has also been observed (albeit
381 in reduced form) in *H. eriocheir*, the type species of the Hepatosporidae (Stentiford et al.
382 2011). This feature was not reported by Azevedo (1987) for *A. portucalensis*, providing
383 further support that *P. carcini* and *A. portucalensis* are separate.

384

385 Because of these differences, and in the absence of DNA sequence data for *A.*
386 *portucalensis*, we propose that *P. carcini* is the type species of a novel genus
387 (*Parahepatospora*) with affinities to both *Hepatospora* (*Hepatosporidae*) and members of the
388 *Enterocytozoonidae*. However, given the propensity for significant morphological plasticity in
389 some microsporidian taxa (Stentiford et al. 2013b), we note that this interpretation may
390 change in light of comparative DNA sequence data becoming available for *A. portucalensis*.

391

392 5.2 Could *Parahepatospora carcini* n. gen n. sp belong within the *Hepatosporidae* (Stentiford
393 et al. 2011)?

394 The *Hepatosporidae* was tentatively proposed to contain parasites infecting the
395 hepatopancreas of crustacean hosts (Stentiford et al. 2011). To date, it contains a single
396 taxon, *H. eriocheir*, infecting Chinese mitten crabs (*Eriocheir sinensis*) from the UK
397 (Stentiford et al. 2011), and from China (Wang et al. 2007). The *Hepatosporidae* (labelled
398 within Fig. 5) is apparently a close sister to the *Enterocytozoonidae*. As outlined above, *P.*
399 *carcini*, *H. eriocheir* and all members of the *Enterocytozoonidae* share the developmental
400 characteristic of early spore organelle formation (such as the polar filament and anchoring
401 disk) within the pre-divisional sporont plasmodium. In contrast, members of the
402 *Enterocytozoonidae*-like clade display developmental features consistent with all other known

403 microsporidian taxa (i.e. spore precursor organelles form after the separation of the sporont
404 from the plasmodium, Rode et al. 2013). Like *H. eriocheir*, *P. carcini* displays early spore-
405 organelle formation both pre- and post- sporont separation from the sporont plasmodium. It
406 is tempting to propose that this characteristic is an intermediate trait between the
407 Enterocytozoonidae and all other Microsporidia and, that this trait is possibly definitive for
408 members of the Hepatosporidae; but further SSU rRNA gene phylogeny data is required to
409 further confirm this, and to link these observations. Intriguingly, *Agmasoma penaei*
410 (branching below *P. carcini*), a pathogen of the muscle and gonad (only gonad in type host),
411 which is closely associated to *P. carcini* phylogenetically (Fig. 5-6), shows tubular inclusions
412 at the plasmodium developmental stage; however polar filament precursors do not fully
413 develop until after sporont division (Sokolova et al. 2015); this could indicate a further
414 remnant of the developmental pathways seen in *P. carcini*, *H. eriocheir* and members of the
415 Enterocytozoonidae.

416

417 The shared developmental and pathological characteristics of *P. carcini* and *H. eriocheir*
418 suggest a taxonomic link; however this is not clearly supported by the SSU rRNA gene
419 phylogenies (Fig. 5 & 6). Confidence intervals supporting the placement of *P. carcini* outside
420 of both the Enterocytozoonidae, the Enterocytozoon-like clade and the Hepatosporidae are
421 low (Fig. 5 & 6) forcing us to suggest that additional data in the form of further gene
422 sequencing of this novel parasite, or possibly from others more closely related through
423 diversity studies, is required before confirming a familial taxonomic rank for this new taxon.

424

425 5.3 Is *Parahepatospora carcini* n. gen. n. sp. an invasive pathogen or novel acquisition?

426 The 'enemy release' concept proposes that invasive hosts may benefit from escaping their
427 natural enemies (including parasites) (Colautti et al. 2004). Invasive species may also
428 introduce pathogens to the newly invaded range, as illustrated by spill-over of crayfish
429 plague (Jussila et al. 2015) to endangered native crayfish in Europe. Invaders can also
430 provide new hosts for endemic parasites through parasite acquisition (e.g. Dunn and
431 Hatcher, 2015).

432

433 Invasive populations of *C. maenas* in Canada are thought to have originated from donor
434 populations in Northern Europe, specifically: Scandinavia, the Faroe Islands and Iceland,
435 based on microsatellite analysis (Darling et al. 2008). *Carcinus maenas* are yet to be
436 screened for microsporidian parasites within these ancestor populations and they may prove
437 to be a good geographic starting point for studies to screen for *P. carcini*. Alternatively, the
438 recent discovery of *P. carcini* at low prevalence in *C. maenas* from the invasive range in
439 Canada could indicate that the parasite has been acquired from the Canadian environment

440 via transfer from an unknown sympatric host. The low prevalence (a single infected
441 specimen) of infection could suggest the single *C. maenas* in this study was infected
442 opportunistically, however the potential remains for *P. carcini* to be present at low
443 prevalence, with gross pathology, as a mortality driver and emerging disease in *C. maenas*
444 on the Canadian coastline. Currently, no evidence is available to confirm whether *P. carcini*
445 is non-native or endemic.

446

447 For future studies it is important to consider whether *P. carcini* may be a risk to native wildlife
448 (Roy et al. 2016), or, if the parasite has been acquired from the invasive range (pathogen
449 acquisition), how it was acquired. If invasive, important questions about the invasion
450 pathway of *P. carcini* would help to indicate its risk and invasive pathogen status (Roy et al.
451 2016). Finally, assessing the behavioural and life-span implications of infection could
452 address whether *P. carcini* has the potential to be used to control invasive *C. maenas* on the
453 Canadian coastline (potential biological control agent).

454

455

456 **Acknowledgements:**

457 This work was supported by NERC funding to AMD, a NERC CASE studentship (case
458 partner CEFAS) to JB (Award #: 1368300), Cefas contract DP227X to GDS and the Atlantic
459 Lobster Sustainability Foundation (Canada). Thanks to Brad Elliott (Dalhousie University),
460 Stephanie Hall (Dalhousie University) and Rory Clark for their help in collecting and
461 dissecting crabs. Further thanks to Stuart Ross and Kelly Bateman for their help in ultra-thin
462 sectioning for electron microscopy and Matthew Green for histological and chemical
463 transport advice. Invasive green crabs were collected in Malagash, Nova Scotia, Canada
464 under a Department of Fisheries and Oceans Canada Scientific licence: SG-RHQ-144-068.

465

466

467 **References**

468

469 Azevedo, C. (1987). Fine structure of the microsporidian *Abelspora portucalensis* gen. n., sp.
470 n. (Microsporidia) parasite of the hepatopancreas of *Carcinus maenas* (Crustacea,
471 Decapoda). *Journal of Invertebrate Pathology*, 49(1), 83-92.

472

473 Balbiani, G. (1882). Sur les microsporidies ou psorospermies des articules. *CR Acad. Sci*,
474 95, 1168-1171.

475

476 Bateman, K. S., Wiredu-Boakye, D., Kerr, R., et al., (2016). Single and multi-gene phylogeny
477 of Hepatospora (Microsporidia)-a generalist pathogen of farmed and wild crustacean hosts.
478 Parasitology, 143(8), 971-982.
479

480 Bright, C. (1999). Invasive species: pathogens of globalization. Foreign Policy, 116, 50-64.
481

482 Capella-Gutiérrez, S., Marcet-Houben, M., & Gabaldón, T. (2012). Phylogenomics supports
483 microsporidia as the earliest diverging clade of sequenced fungi. BMC biology, 10(1), 47.
484

485 Colautti, R. I., Ricciardi, A., Grigorovich, I. A., et al., (2004). Is invasion success explained by
486 the enemy release hypothesis?. Ecology Letters, 7(8), 721-733.
487

488 Clotilde-Ba, F. L., and Toguebaye, B. S. (1994) Ultrastructure and Development of
489 Agmasoma penaei (Microspora, Thelohaniidae) found in Penaeus notialis (Crustacea,
490 Decapoda, Penaeidae) from Senegal. European Journal of Protistology, 30, 347-353.
491

492 Corsaro, D., Walochnik, J., Venditti, D., et al. (2014). Microsporidia-like parasites of
493 amoebae belong to the early fungal lineage Rozellomycota. Parasitology research, 113(5),
494 1909-1918.
495

496 Darling, J. A., Bagley, M. J., Roman, J. O. E., et al., (2008). Genetic patterns across multiple
497 introductions of the globally invasive crab genus Carcinus. Molecular Ecology, 17(23), 4992-
498 5007.
499

500 Dunn, A. M., & Hatcher, M. J. (2015). Parasites and biological invasions: parallels,
501 interactions, and control. Trends in parasitology, 31(5), 189-199.
502

503 Haag, K. L., James, T. Y., Pombert, J. F., et al. (2014). Evolution of a morphological novelty
504 occurred before genome compaction in a lineage of extreme parasites. Proceedings of the
505 National Academy of Sciences, 111(43), 15480-15485.
506

507 Hopwood, D., (1996). Theory and practice of histopathological techniques. In: Bamcroft,
508 J.D., Stevens, A. (Eds.), Fixation and Fixatives, fourth ed. Churchill Livingstone, Hong Kong,
509 pp. 23–46.
510

511 Jussila, J., Vrezec, A., Makkonen, J., et al., (2015). Invasive crayfish and their invasive
512 diseases in Europe with the focus on the virulence evolution of the crayfish plague.

513 Biological invasions in changing ecosystems: vectors, ecological impacts, management and
514 predictions. De Gruyter Open, Berlin, pp.183-211.
515

516 Karpov, S. A., Mamkaeva, M. A., Aleoshin, V. V., et al., (2015). Morphology, phylogeny, and
517 ecology of the aphelids (Aphelidea, Opisthokonta) and proposal for the new superphylum
518 Opisthosporidia. Roles and mechanisms of parasitism in aquatic microbial communities, 5,
519 64-74.
520

521 Katoh, K., Standley, D.M., (2013). MAFFT multiple sequence alignment software version 7:
522 improvements in performance and usability. Mol. Biol. Evol. 30, 772-780.
523

524 Reynolds, E.S., 1963. The use of lead citrate at high pH as an electron-opaque stain in
525 electron microscopy. J. Cell Biol. 17, 208–212.
526

527 Rode, N. O., Landes, J., Lievens, E. J., et al., (2013). Cytological, molecular and life cycle
528 characterization of *Anostracospora rigaudi* ng, n. sp. and *Enterocytospora artemiae* ng, n.
529 sp., two new microsporidian parasites infecting gut tissues of the brine shrimp *Artemia*.
530 Parasitology, 140(9), 1168-1185.
531

532 Ronquist F., Teslenko M., van der Mark P., et al. (2012). MrBayes 3.2: efficient Bayesian
533 phylogenetic inference and model choice across a large model space. Syst. Biol. 61, 539-42.
534

535 Roy, H. E., Hesketh, H., Purse, B. V. et al. (2016). Alien Pathogens on the Horizon:
536 Opportunities for Predicting their Threat to Wildlife. Conservation Letters. In Press.
537

538 Sokolova, Y., Pelin, A., Hawke, J., & Corradi, N. (2015). Morphology and phylogeny of
539 *Agmasoma penaei* (Microsporidia) from the type host, *Litopenaeus setiferus*, and the type
540 locality, Louisiana, USA. International journal for parasitology, 45(1), 1-16.
541

542 Sprague, V., & Couch, J. (1971). An Annotated List of Protozoan Parasites, Hyperparasites,
543 and Commensals of Decapod Crustacea*. The Journal of Protozoology, 18(3), 526-537.
544

545 Stamatakis, A. (2014). RAxML Version 8: A tool for Phylogenetic Analysis and Post-Analysis
546 of Large Phylogenies. Bioinformatics, 30, 1312-1313.
547

548 Stentiford, G. D., Bateman, K. S., Dubuffet, A., et al., (2011). *Hepatospora eriocheir* (Wang
549 and Chen, 2007) gen. et comb. nov. infecting invasive Chinese mitten crabs (*Eriocheir*
550 *sinensis*) in Europe. *Journal of invertebrate pathology*, 108(3), 156-166.

551

552 Stentiford, G. D., Feist, S. W., Stone, D. M., et al., (2013a). Microsporidia: diverse, dynamic,
553 and emergent pathogens in aquatic systems. *Trends in parasitology*, 29(11), 567-578.

554

555 Stentiford, G. D., Bateman, K. S., Feist, S. W., et al., (2013b). Plastic parasites: extreme
556 dimorphism creates a taxonomic conundrum in the phylum Microsporidia. *International*
557 *journal for parasitology*, 43(5), 339-352.

558

559 Stentiford, G. D., Becnel, J. J., Weiss, L. M., et al., (2016). Microsporidia–Emergent
560 Pathogens in the Global Food Chain. *Trends in Parasitology*, 32(4), 336–348.

561

562 Tourtip, S., Wongtripop, S., Stentiford, G. D., et al., (2009). *Enterocytozoon hepatopenaei*
563 sp. nov. (Microsporidia: Enterocytozoonidae), a parasite of the black tiger shrimp *Penaeus*
564 *monodon* (Decapoda: Penaeidae): Fine structure and phylogenetic relationships. *Journal of*
565 *invertebrate pathology*, 102(1), 21-29.

566

567 Vávra, J., Hyliš, M., Fiala, I., et al., (2016). *Globulispora mitoportans* ng, n. sp.,
568 (Opisthosporidia: Microsporidia) a microsporidian parasite of daphnids with unusual spore
569 organization and prominent mitosome-like vesicles. *Journal of invertebrate pathology*, 135,
570 43-52.

571

572 Vossbrinck, C. R., & Debrunner-Vossbrinck, B. A. (2005). Molecular phylogeny of the
573 Microsporidia: ecological, ultrastructural and taxonomic considerations. *Folia Parasitol*, 52(1-
574 2), 131-142.

575

576 Wang, W., & Chen, J. (2007). Ultrastructural study on a novel microsporidian,
577 *Endoreticulatus eriocheir* sp. nov. (Microsporidia, Encephalitozoonidae), parasite of Chinese
578 mitten crab, *Eriocheir sinensis* (Crustacea, Decapoda). *Journal of invertebrate pathology*,
579 94(2), 77-83.

580

581 Wolinska, J., Giessler, S., & Koerner, H. (2009). Molecular identification and hidden diversity
582 of novel *Daphnia* parasites from European lakes. *Applied and environmental microbiology*,
583 75(22), 7051-7059.

584

585

586 **Figures and Tables**

587

588 Figure 1: Histology of a *Parahepatospora carcini* n. gen n. sp. infection in the
589 hepatopancreas of *Carcinus maenas*. a) A cross-section of an hepatopancreatic tubule
590 infected with *P. carcini* (white arrow). The star indicates a blood vessel and 'L' represent the
591 lumen of two tubules. Scale = 50µm. b) A high magnification image of early infected cells.
592 Development of early sporonts occurs as the periphery of the cell cytoplasm (white arrow)
593 and spores appear to aggregate in the centre (black arrow). Scale = 10µm. c) Cells can be
594 seen sloughing from the basal membrane (white arrow) into the lumen, filled with
595 microsporidian spores. Scale = 10µm.

596

597 Figure 2: Transmission electron micrograph of the early developmental stages of
598 *Parahepatospora carcini* n. gen. n. sp. a) Unikaryotic meront with thin cell membrane (white
599 arrow) and single nucleus (N). Scale = 500nm. b) Diplokaryotic meront with connected nuclei
600 (N/N). Scale = 500nm. c) Separation of the nuclei (N) within the diplokaryotic cell in
601 preparation for multinucleate cell formation. Note the darkening of cytoplasm (C) and
602 thickening cell membrane (white arrow). Scale = 500nm. d) Multinucleate plasmodium
603 containing 12 nuclei (N). Scale = 2µm. e) Plasmodium cell division. Individual pre-
604 sporoblasts bud from the main plasmodium (black arrow). Early polar filament and anchoring
605 disks can be seen (white arrow) alongside further cell membrane thickening. Scale = 500nm.
606 f) Sporoblast formation after multinucleate cell division. Each sporoblast contains a single
607 nucleus (N) and polar filament with an anchoring disk (white arrows). Scale = 500nm.

608

609 Figure 3: Final spore development of *Parahepatospora carcini* n. gen. n. sp. a) Sporoblasts
610 of *P. carcini* hold 5-6 turns of the polar filament, a single nucleus and an electron lucent
611 organelle, suspected to develop into the polaroplast (black arrow). Scale = 500nm. b) Cross
612 section of a fully developed spore displaying a single nucleus (N) and 5-6 turns of the polar
613 filament (white arrow). Note the fully thickened, electron lucent endospore (black arrow).
614 Scale = 500nm. c) Cross section of a fully formed spore depicting a single nucleus (N),
615 polaroplast (PP), polar vacuole (PV), cross sections of the polar filament (white arrow) and
616 anchoring disk (black arrow). Scale = 500nm. d) The final spore of *P. carcini* with a
617 membranous polaroplast (white arrow) and curving, right-leaning, polar filament with
618 anchoring disk (black arrows). Note the thinner endospore at the point closest to the
619 anchoring disk. Scale = 500nm.

620

621 Figure 4: Predicted lifecycle of *Parahepatospora carcini* n. gen. n. sp. 1) The lifecycle begins
622 with a uninucleate meront. 2) The nucleus of the meront divides to form a diplokaryotic
623 meront. 3) The diplokaryotic nucleus divides, eventually forming a large meront plasmodium.
624 4) The meront plasmodium shows cytoplasmic invagination before early sporont formation.
625 5) A cytoplasmic elongation from a sporogonial plasmodium coupled with budding sporonts;
626 most with early spore-organelle formation following the primary development pathway. 6)
627 Sporonts equipped with early spore-organelles mature to sporoblasts. 7) Sporonts without
628 early spore-organelles now develop these organelles to become sporoblasts; a secondary,
629 uncommon pathway of development. 8) Sporoblasts mature with further thickening of the cell
630 wall and completely separate from the sporogonial plasmodium. 9) The final, infective,
631 uninucleate spore is formed, completing the lifecycle.

632

633 Figure 5: Bayesian SSU rDNA phylogeny showing the branching position of
634 *Parahepatospora carcini* n. gen. n. sp. in microsporidian clade IV. Both Maximum Likelihood
635 bootstrap values and Bayesian Posterior Probabilities are indicated at the nodes (ML/PP).
636 Nodes supported by >90% bootstrap/0.90 PP are represented by a black circle on the
637 branch leading to the node. The numbered microsporidian clades are indicated to the right of
638 the tree. Important microsporidian families and groups are also highlighted with
639 accompanying colours (Enterocytozoonidae, Enterocytospora-like, Hepatosporidae, etc.).
640 Members of the genus *Glugea* (Clade V) are utilised as an out-group (O/G). Scale = 0.3
641 Units.

642

643 Figure 6: Bayesian SSU rDNA phylogeny showing the branching position of
644 *Parahepatospora carcini* n. gen. n. sp. in microsporidian clade IV alongside microsporidia
645 with available development pathways. Both Maximum Likelihood bootstrap values and
646 Bayesian Posterior Probabilities are indicated at the nodes (ML/PP). Nodes supported by
647 >90% bootstrap/0.90 PP are represented by a black circle on the branch leading to the
648 node. The blue group (Enterocytozoonidae) all utilise large plasmodia with polar-filament
649 development at the pre-sporoblastic divisional level. The yellow group (Hepatosporidae)
650 show precursor development to the aforementioned trait. The orange group
651 (Enterocytospora-like clade) develop the polar filament post-sporoblastic division;
652 considered a conventional microsporidian development method. *Parahepatospora carcini*
653 development is included alongside as an intermediate feature. *Nosema* spp. act as an out-
654 group. Scale = 0.2 Units.

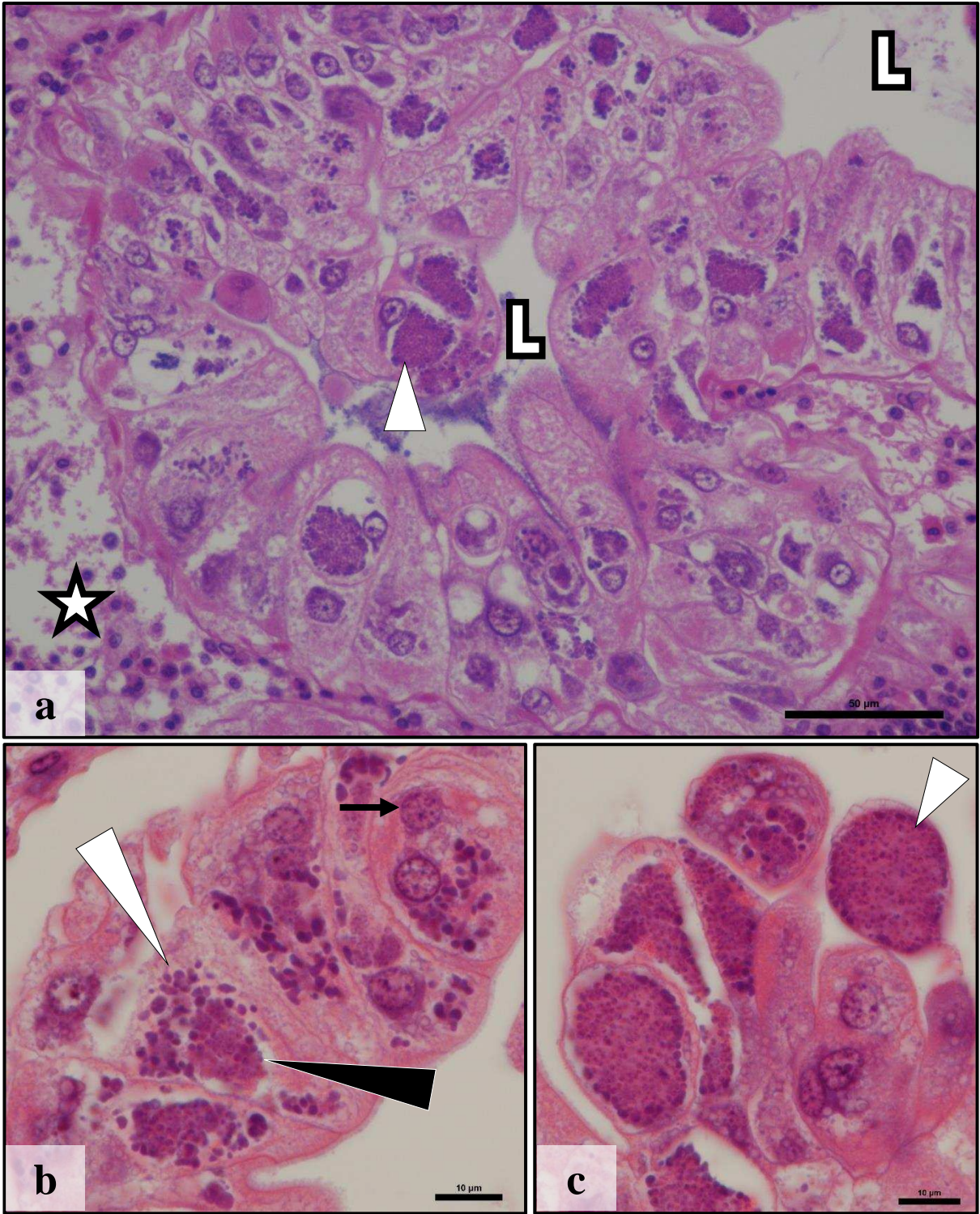


Figure 1

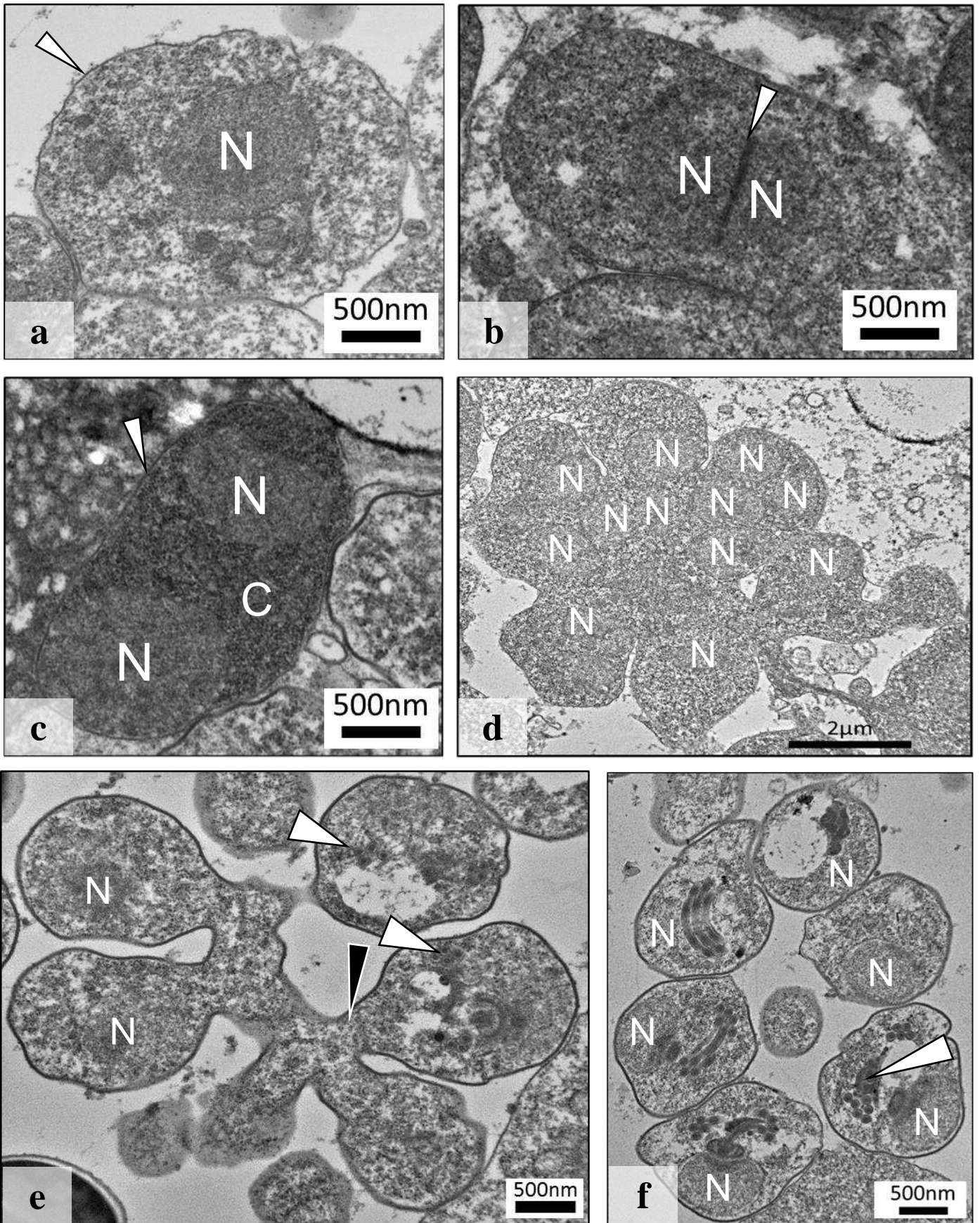


Figure 2

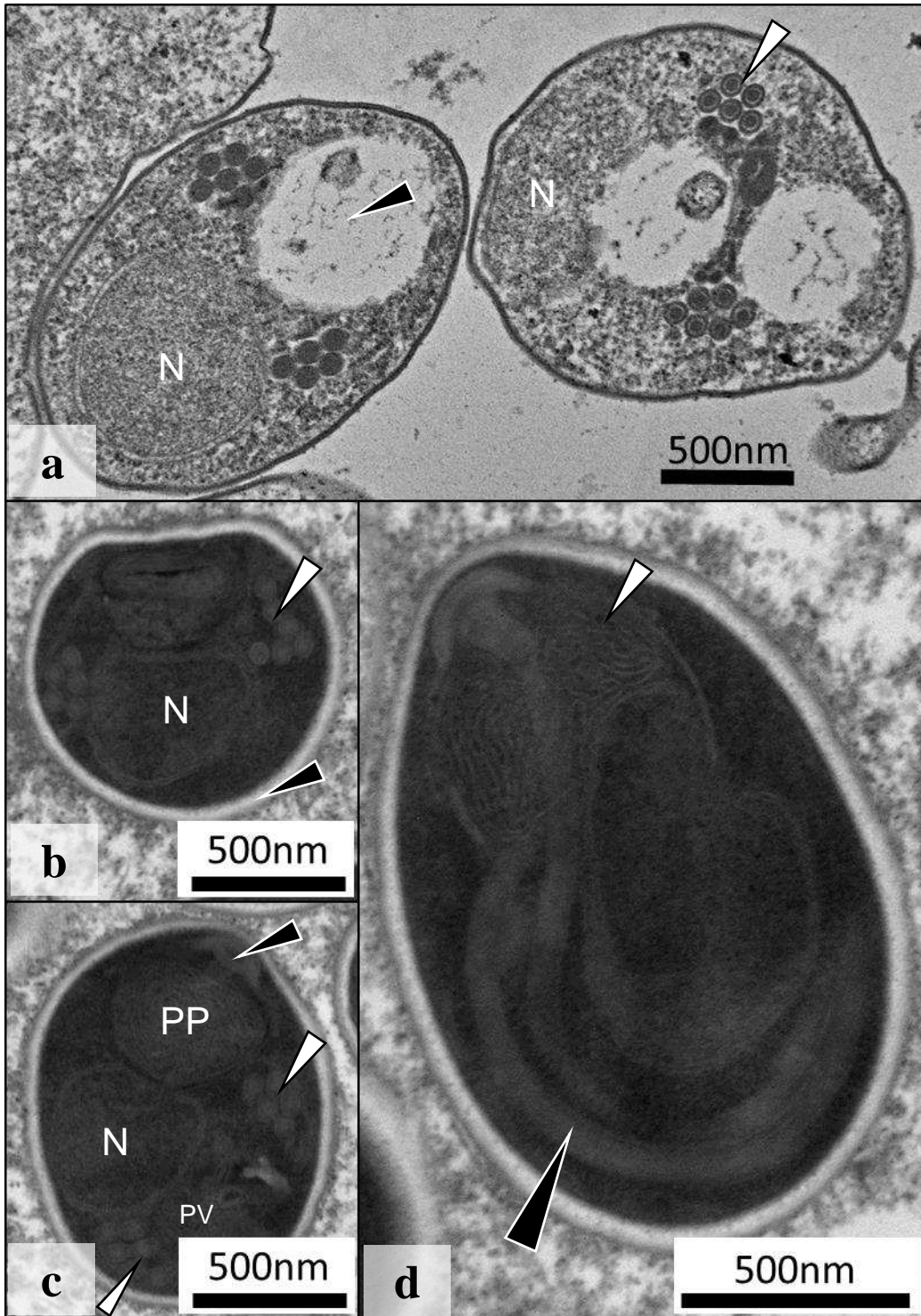


Figure 3

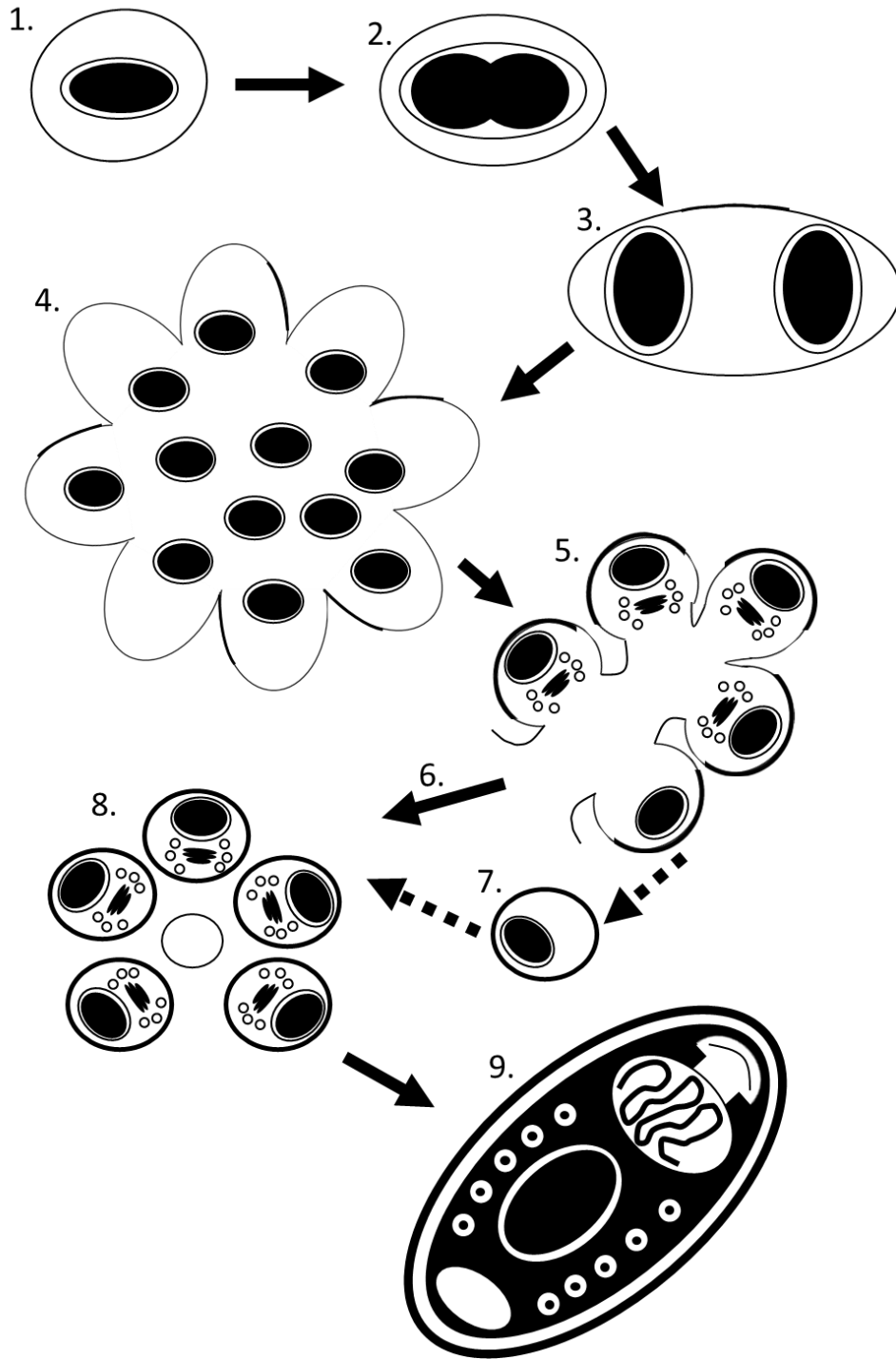


Figure 4

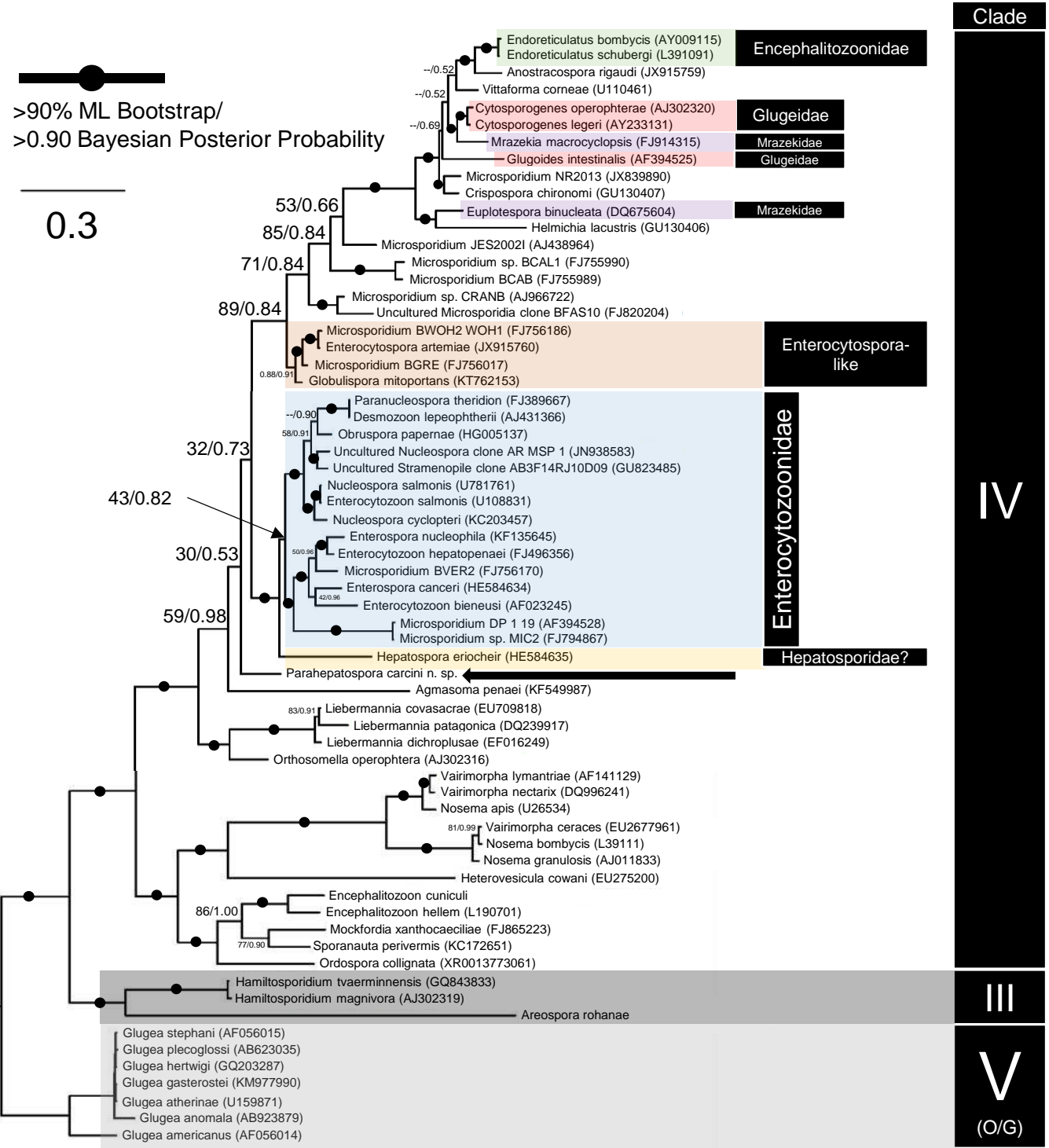


Figure 5

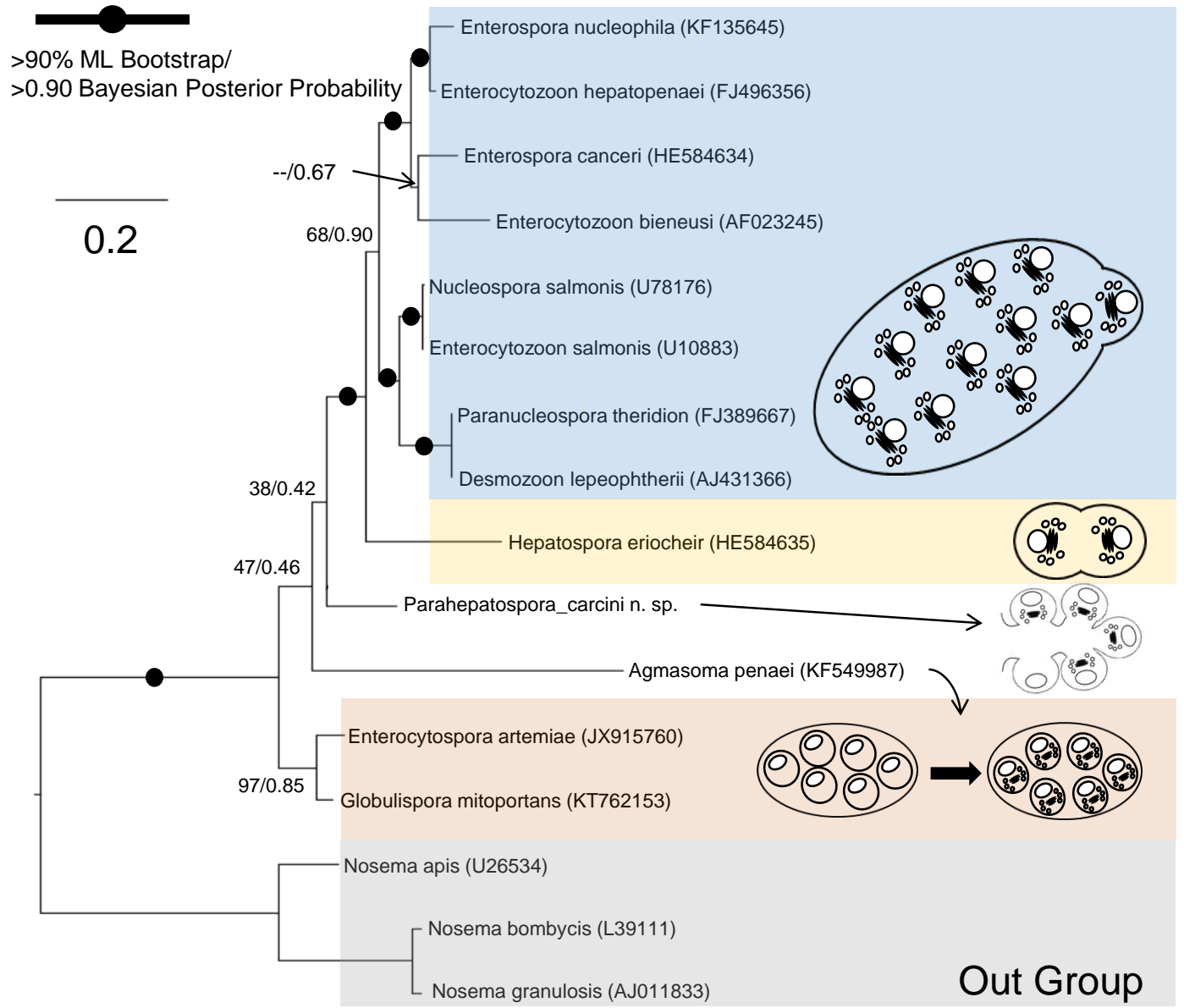


Figure 6